Lower-Tropospheric Ozone (LTO) derived from TOMS near mountainous regions

M. J. Newchurch

Department of Atmospheric Science, University of Alabama in Huntsville and Atmospheric Chemistry Division, National Center for Atmospheric Research, Boulder, Colorado

X. Liu

Department of Atmospheric Science, University of Alabama in Huntsville

J. H. Kim

Department of Atmospheric Science, Pusan National University, South Korea

Abstract. Using Total Ozone Mapping Spectrometer (TOMS) version-7 level-2 clear-sky (reflectivity ≤ 20%) ozone measurements corrected for aerosol effects and sea-glint errors, we derived Lower Tropospheric Ozone (LTO) west and east of the Andes, the Mexican and Rocky Mountains, the mountains in Africa and the Arabian Peninsula, New Guinea, and the Himalayan Mountains. The derived results agree reasonably well with the seasonality of LTO from ozonesonde observations at Boulder, Cristobal, Fiji, Java, and Tahiti. The LTO seasonality found in the biomass burning seasons characterized by the ATSR World Fire Atlas west and east of the Andes (23°S-2°N), east of the Mexican Mountains (15°-23°N), South Sudan (6°-14°N), South Africa (30°-28°S), and west of New Guinea is consistent with the influence of biomass burning on the formation of tropospheric ozone in these regions. The significant El Niño influence on LTO west of New Guinea is evident throughout several El Niño cycles. The spring maximum in ozone west of the Mexican Mountains, in western China, and west of the Andes (32°-23°S) is consistent with a stratospheric intrusion source. East of the Mexican Mountains (23°-30°N), both west and east of the Rocky Mountains, in north Sudan and Iraq, and in western China, high concentrations of ozone are found in these continental and coastal regions which are affected by anthropogenic sources. The maximum ozone in these regions usually occurs in the summer due to photochemical ozone production. A summer LTO minimum occurs in coastal regions west of the Andes and west of Mexico, due to ozone destruction in low NO_x and high H_2O marine environment. A summer minimum also occurs in south Sudan in the rainy season. The LTO in the northern tropics of South America (4°-10°N), Africa (1°S-2°N), and east of New Guinea (7°-3°S) experiences little seasonal variation.

1. Introduction

Tropospheric ozone plays a key role in the chemical processes and energy budget of the troposphere [*Brasseur et al.*, 1998; *Crutzen*, 1988]. The tropospheric OH radical, formed mainly by the photolysis of ozone, also controls the lifetimes of a large number of gases [*Cunnold et al.*, 1997]. Ozone is also an important greenhouse gas and is associated with air pollution such as vehicle emission, fuel combustion [*Jacob et al.*, 1994], and biomass burning [*Thompson et al.*, 1996b]. Furthermore, sources in one region can have global impacts [*Jacob et al.*, 1999]. The increase of tropospheric ozone is of great concern also due to its deleterious effects on human health and vegetation. Because of the sparse distribution of ground-based ozone observations and the large

spatial and temporal variability of tropospheric ozone, satellite remote sensing techniques are crucial for studying the global distributions, sources and sinks, transport, seasonal behavior, and trends of tropospheric ozone.

Biomass burning is an important source of tropospheric ozone especially in South America, Africa, and east Asian regions. Using a global circulation model, *Marufu et al.* [2000] estimated that biomass burning accounts for 24% of the ozone in the boundary layer with a large uncertainty of 70% over Africa. *Moxim and Levy* [2000] also showed that biomass burning can account for about 30% of the ozone in the boundary layer over the Atlantic Ocean.

Jiang and Yung [1996] introduced the Topographic Contrast Method (TCM) for deriving Lower Tropospheric Ozone (LTO) by subtracting the Total Ozone Mapping Spectrometer (TOMS) Total Column Ozone (TCO) over the Andes from the TCO over the eastern Pacific Ocean. *Kim and Newchurch* [1996] applied this method to study the LTO over the west and east sides of the Andes and over New Guinea. These studies found trends with significant increases of approximately 1%/yr in the eastern Pacific Ocean and west of

New Guinea, which appeared to be associated with increases in biomass burning in South America and New Guinea. These studies analyzed gridded (level 3) version-7 (V7) TOMS observations.

The Level-3 data, including clear, cloudy, and partially cloudy observations, are interpolated to a fixed latitude/longitude grid and are not corrected for aerosol or sea-glint effects. Although the V7 algorithm corrected some ozone retrieval errors associated with low clouds in the version-6 algorithm [*Hsu et al.*, 1997; *McPeters and Labow*, 1996], ozone retrieval errors remain due to using the monthly mean International Satellite Cloud Climatology Project (ISCCP) cloud climatology [*Newchurch et al.*, 2001] and due to sun glint and tropospheric aerosols [*Torres and Bhartia*, 1999]. Because *Jiang and Yung* [1996], and *Kim and Newchurch* [1996, 1998] used the gridded level-3 data, errors associated with clouds, aerosols, and sun glint along with the less precise gridded data representation could affect the accuracy of the derived LTO.

In this study we derive LTO from V7 TOMS level-2 (discrete point, not gridded [*McPeters et al.*, 1996]) clear scene measurements (reflectivity $\leq 20\%$) corrected for aerosol and sea-glint effects around several mountainous regions, including the Andes, the Mexican, and the Rocky Mountains, New Guinea, the Himalayan Mountains, and the mountains in Africa and the Arabian Peninsula. We compare the derived LTO with ozonesonde measurements at Boulder, Cristobal, Fiji, Tahiti, and Java and analyze the seasonal behavior of LTO in these regions.

2. Data and Methodology

To derive LTO, we used the high-resolution V7 TOMS level-2 data from November 1978 to May 1993 Nimbus 7 (N7) and from July 1996 to December 1999 Earth Probe (EP) observations. Only clear-sky measurements with reflectivity less than 20% were used to avoid retrieval errors associated with clouds. The Dave reflectivity correction code is used to correct errors due to tropospheric aerosols and sun glint (C. G. Wellemeyer, personal communication, 1999) (herein after referred to as W99). Departures from the Rayleigh atmosphere assumed in construction of the radiance tables used to derive total ozone tend to display a wavelength dependence that is linear in derived surface reflectivity. The Dave correction assumes that the residues of the triplet ozone retrieval are due to an error in the ozone associated with such a linear dependence in reflectivity. This Dave correction provides a good correction for the impact of sun glint and tropospheric aerosols in the V7 TOMS data, consistent with the results of *McPeters et al.* [1996] and *Torres and Bhartia* [1999] within 1% (W99). The Electrochemical Concentration Cell (ECC) ozonesonde observations at Boulder (40°N, 105°W, from WMO/World Ozone Data Center), the Southern Hemisphere ADditional OZonesonde (SHADOZ) measurements [*Thompson and Witte*, 1999; Thompson et al., The 1998-2000 SHADOZ (Southern Hemisphere Additional Ozonesondes) Tropical Ozone Climatology: Comparison with TOMS and Ground-based Measurements, submitted to *J. Geophys. Res.*, 2001] at Cristobal (1°S, 90°W), Fiji (18°S, 178°W), Tahiti (18°S, 149°W), and Java (7.5°S, 112.6°E), and Electrochemical Carbon-iodine ozonesonde measurements at Java [*Fujiwara et al.*, 2000] provide a validation reference for our derived LTO. The effects of

biomass burning on LTO derive from the global fire count data in 1998 from the ATSR World Fire Atlas (http://shark1.esrin.esa.it/ionia/FIRE/AF/ATSR/). Because these fire counts result from the 3.7 μm channel of ATSR-2 nighttime images, with a brightness temperature greater than 312 K considered a fire count, these data mainly reflect saturated fire pixels and underestimate the true fire counts.

We define mountain regions with terrain pressure less than 800 hPa between 40°S and 40°N latitude. Figure 1 shows the available locations where we applied TCM, including the Andes Mountains (38°S-10°N), the Mexican and Rocky Mountains (15°N- 40°N), New Guinea (7°S-3°S), the Himalayas (28°N-40°N), and some regions in Africa and the Arabian Peninsula. Most of these locations contain relatively narrow longitudinal mountain extents. When the mountains are too broad, such as the Himalayas, we instead found the mountain edges with terrain pressure less than 800 hPa on both sides. The daily average TCO at mountain levels results from using all available measurements with terrain pressure less than 800 hPa within ±1° longitude and 1° latitude of the mountain peak. On both east and west sides of mountains we obtained the corresponding TCO, using measurements with terrain pressure greater than 950 hPa within ±7.5° longitude. Using a somewhat smaller longitude range shows little effect on the derived results. To compare the magnitude of derived LTO across all locations, it is convenient to express the LTO in mixing ratio rather than ozone column. Assuming a well-mixed LTO and hydrostatic atmosphere, we calculate the LTO mixing ratio using the difference between TCO at the mountain level (ML) and at the sea level (SL):

$$O_3 \text{ (ppbv)} = 1.25 \times \frac{TCO\ (s) - TCO\ (m)}{P(s) - P(m)} \tag{1}$$

$TCO(s)$ and $TCO(m)$ are the daily average TCO (Dobson Units (DU)) at SL and ML, respectively; $P(s)$ and $P(m)$ are the average terrain pressure (atm) at SL and ML, respectively. The mountain terrain pressures at these locations range from 800 hPa to 530 hPa, with an average of 720 hPa (about 3 km in height). Due to requiring only clear-sky measurements, we might not obtain the daily ozone mixing ratio every day. In this case, the average of TCO at ML or SL within ±1° latitude and ±2 days provides the ozone mixing ratio.

An important assumption in the TCM is that both stratospheric ozone and upper-tropospheric ozone (defined here as the ozone amount between the ML and the tropopause) are the same over both the mountain and the adjacent land (or ocean). The derived daily LTO shows large variability from day to day, and some ozone mixing ratios are negative or extremely large, suggesting the assumption might not be correct on a daily bias. To reduce this variability on the derived LTO, we formed the monthly mean ozone mixing ratio by requiring at least 10 daily values from 15° S-15° N and at least 15 values at the other latitudes. Because the natural variability of ozone is about 30% of the monthly mean in middle latitudes, and smaller in tropical regions [*World Meteorological Organization (WMO)*, 1999], we omit these monthly mean values with a relative standard error greater than 30% or with standard deviations greater than 10 ppbv.

In the TOMS V7 algorithm the radiance at ML is interpolated from those calculated at 1.0 and 0.4 atm pressure levels. This radiation interpolation introduces ozone retrieval errors that are small in the retrieved TCO but are significant
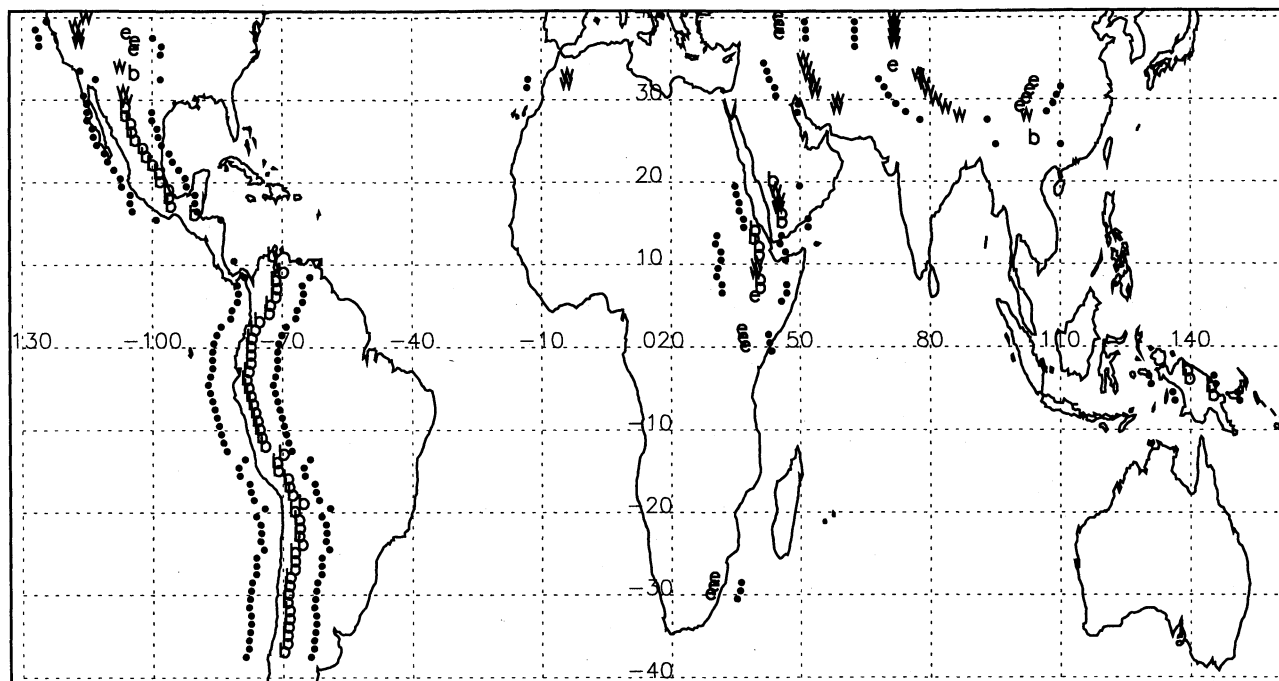
Figure 1. Locations where the Topographic Contrast Method derives lower-tropospheric ozone: Figures 1w, 1e, and 1b indicate that we derive lower tropospheric ozone on west side only, east side only, or both sides of mountain regions, respectively. The dots are ±7.5° in longitude from the corresponding mountainous locations.

in LTO. We used the TOMS radiative transfer code (TOMRAD, the forward model of TOMS algorithm), and the TOMS V7 algorithm to investigate the radiation interpolation errors for clear-sky measurements at elevated surface levels. For the low-latitude ozone profile containing a total ozone column of 275 DU and surface reflectivity of 8%, we used TOMRAD to calculate the radiances for surface pressure of 1.0 atm and 0.75 atm and then inverted these radiances with the TOMS V7 algorithm to retrieve the total ozone. The retrieved ozone for 1.0 atm is almost exactly 275 DU, consistent with the input total ozone. However, the retrieved TCO at 0.75 atm is only 265.3 DU at nadir conditions, 3.5 DU smaller than the expected total ozone from the TOMS standard ozone profile. This underestimation of ozone at elevated surfaces decreases slightly with increasing viewing geometry. It also varies with the surface pressure and peaks at about 700 hPa. The radiation interpolation errors also occur over cloudy conditions (reflectivity ≥ 80%) [*Newchurch et al.*, 2001] but with an opposite sign. The underestimation in TCO above ML would increase LTO by 10~20 ppbv depending on the viewing geometry and mountain heights. The results in this paper have been corrected for this interpolation error. The TOMS sensor is not as sensitive to LTO [*Klenk et al.*, 1982; *Hudson et al.*, 1995] as it is to stratospheric ozone. The average ozone retrieval efficiency factor in the lower troposphere (0~3 km) is ~0.5 for clear-sky conditions [*Hudson et al.*, 1995]. However, applying the retrieval efficiency correction to the derived LTO requires knowledge of the actual climatology, an unknown quality for most of the study areas. Therefore, we have not applied any correction for the efficiency factor. This study emphasizes the seasonal behavior of derived LTO, which agrees reasonably well with ozonesonde observations.

3. Results and Discussion

3.1. Comparison with Ozonesonde Observations

The monthly mean mixing ratio below the nearby mountain-top altitude obtained from no fewer than two ozonesonde observations provides a good metric for assessing the character of these TCM ozone columns. Figure 2a shows the comparison of the TCM results east of the Rocky Mountains with the ozonesonde observations at Boulder. The derived ozone mixing ratios are limited to the summer season because of the variability constraint. In only 3 of the 15 months is the difference between the TCM and the integrated ozonesonde observations larger than 15 ppbv. These differences could be due to some limitation in our method at midlatitudes, the large ozone variability at midlatitudes, or the natural variability resulting from having a few observations for each month. Except for these 3 months the TCM results agree well with ozonesonde observations within 10 ppbv and show similar annual variability. The LTO results at Andes and New Guinea agree quite well with ozonesonde measurements at Cristobal, Tahiti, New Guinea, and Java in the seasonal behavior.

Figures 2b-2e show the comparison of TCM results with some of the SHADOZ stations. The Cristobal station is at the same latitude and only 5° west of the TCM location. On average, the TCM results are 5 ppbv larger, and they agree quite well with the seasonal variation of LTO at Cristobal. Although the TCM locations west of New Guinea and east of New Guinea are some distance away from the ozonesonde stations at Java and Fiji, our results show good consistency in seasonal variation with ozonesonde data. The TCM results are 0.7 ppbv larger than ozonesonde measurements at Fiji and 5.3 ppbv less than ozonesonde measurements at Java. In Figure
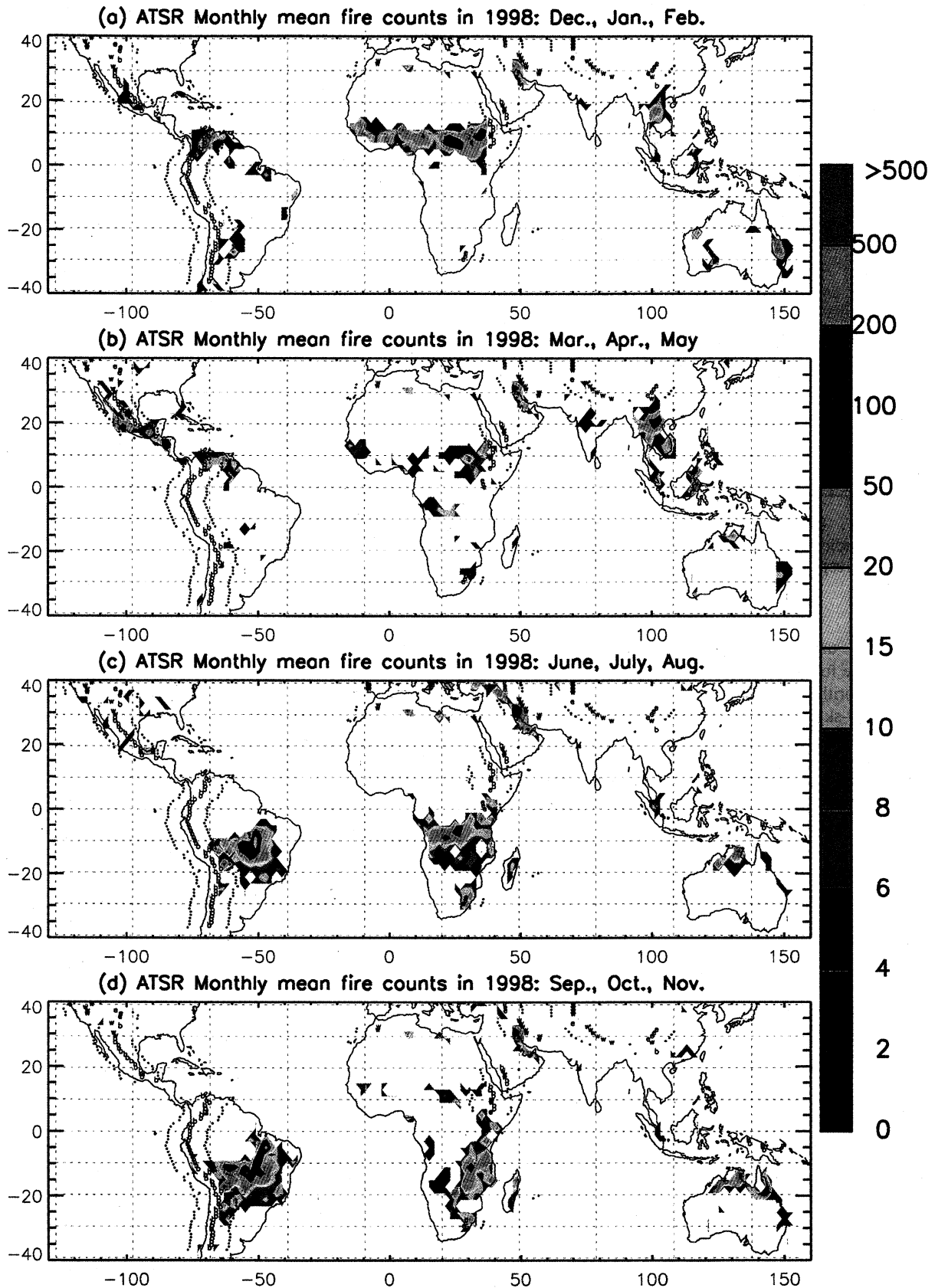
Plate 1. Seasonal fire counts derived from ATSR observations for December-February in Plate 1a through September-November in Plate 1d, respectively. ATSR data are courtesy of ATSR World Fire Atlas Team at ESA/ESRIN.
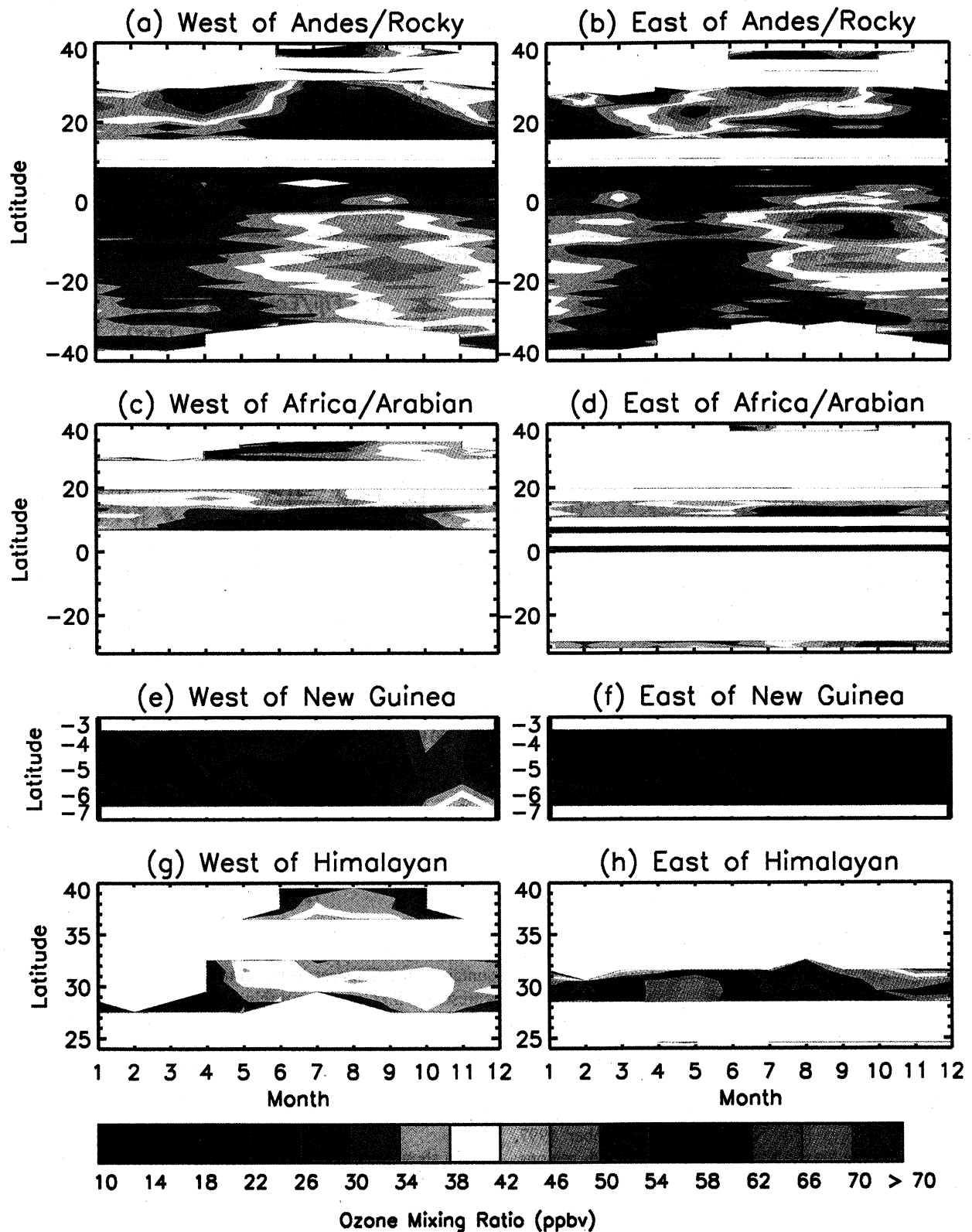
Plate 2. Temporal variation of monthly mean Lower-Tropospheric Ozone (LTO in ppbv) from NIMBUS-7 TOMS (November 1978-May 1993) and Earth Probe TOMS (July 1996-December 1999). (a) LTO west of the Andes, Mexican, and Rocky Mountains. (b) LTO east of those same mountains shown in Plate 2a. (c, d) LTO west and east, respectively, of mountains in Africa and the Arabian Peninsula. (e, f) LTO west and east, respectively, of New Guinea. (g, h) LTO west and east, respectively, of the Himalayas.
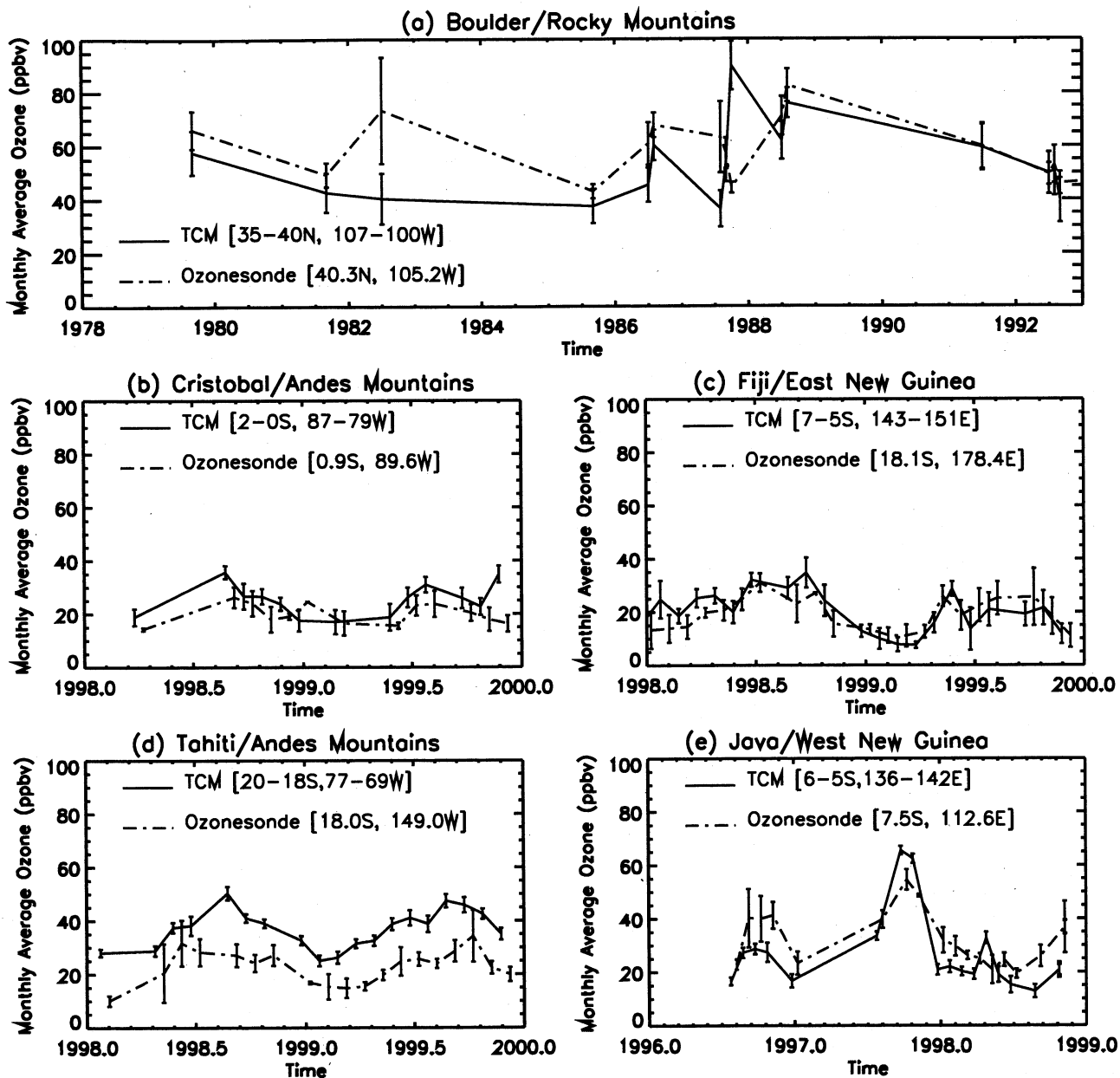
Figure 2. Comparisons of the derived Lower-Tropospheric Ozone (LTO in ppbv) with ozonesonde observations at (a) Boulder/Rocky Mountains, (b) Cristobal/Andes Mountains, (c) Fiji/east New Guinea, (d) Tahiti/Andes Mountains, and (e) Java/west of New Guinea. Error bars represent 1 S.D. of the monthly means. The Boulder data are courtesy of NOAA/CMDL; Cristobal, Fiji, Tahiti, and Java (in 1998) data are courtesy of SHADOZ/GSFC; Java data (before 1998) are courtesy of Fujiwara Masatomo and Shuji Kawakami.

2e, enhanced ozone is observed in both ozonesonde measurements at Java and TCM results in October 1997, concurrent with significant biomass burning in both regions. In Figure 2d the ozonesonde measurements were made at Tahiti, which is in the eastern Pacific Ocean and about 75° away from the LTO locations. Particularly at Tahiti, where the LTO observations are 15 ppbv larger than the Tahiti sondes, one would expect the sonde observations to be lower than the continental observations, because of the significant ozone sink at the sea surface [*Crutzen*, 1988; *Johnson et al.*, 1990], which would decrease the LTO relative to values closer to the continental source regions. Considering these effects, the TCM results agree well with the ozonesonde observations.

3.2. Seasonal Variation of Lower Tropospheric Ozone

To show the seasonal behavior of the LTO, we present the 18-year TOMS average of the monthly mean (minimum of 6 out of 18 years required at each location) ozone mixing ratios. The derived ozone mixing ratios near the Andes from EP TOMS are about 5 ppbv smaller than those from N7, with smaller difference at other locations. An offset in the opposite sense in TCO between EP and N7 (EP ~5DU higher) has been noticed by other researchers and is not understood [*Ziemke and Chandra*, 1999]. Because the LTO is the difference of measurements made by the same instrument and we have no evidence to prefer one instrument to the other, we include data from both EP and N7 periods to calculate the average

climatology. In any event, the LTO from N7 and EP shows similar seasonal behavior. Furthermore, the average of 18-years of results presented below could ameliorate some abnormally high or low LTO values, especially at higher latitudes, due to a local failure in the assumption of constant column ozone above the mountain level between the mountainous region and the sea level regions.

To provide context for the formation of LTO and its seasonal behavior, we present the monthly mean fire count map (2° longitude by 2° latitude) derived from ATSR-2 night images in four seasons in 1998 in Plate 1 (from http://shark1.esrin.esa.it/ionia/FIRE/AF/ATSR/) with superimposed LTO locations from Figure 1. Most of the features are similar to the seasonal behavior observed by *Hao and Liu* [1994]. The biomass burning season in South Africa and South America starts in June-August and ends in September-October. In northern equatorial Africa (0°-15°N), biomass burning peaks in the December-February period. In Mexico, Central America, northern South America, and southeastern Asia, biomass burning peaks in the March-May period. The biomass burning distribution in 1997 was similar in South America, South Africa, and central Africa; however, burning in the other mentioned regions was much weaker. In Indonesia and New Guinea, significantly larger fire counts with a magnitude of 100~500 were observed in September - November 1997.

Plate 2a shows LTO west of the Andes and Rocky Mountains, and the values east of the mountains appear in Plate 2b. The LTO in the eastern Pacific Ocean (2°N-32°S) peaks during the austral late winter and spring (from August to November), with the peaks shifting toward the summer at more southerly latitudes. The minimum LTO occurs 6 months out of phase with the maximum in a clear annual cycle. The LTO derived east of the Andes (i.e., over the continental regions) also peaks during the austral late winter and spring at 4°N-23°S and during the austral summer at 23°S-32°S and is lowest in the fall. Contrary to the constant phase shift west of the Andes, the east-side phase separation between minimum and maximum increases from 5 months at the equator to 8 or 9 months at 30°S. The seasonal behavior of LTO west of the Andes is consistent with the results of *Jiang and Yung* [1996] and *Kim and Newchurch* [1996, 1998]. They analyzed the LTO at 5°-6°S on both sides of the Andes using TOMS level-3 data and arrived at the same seasonal pattern, with the ozone minimum west of the Andes about 2 months earlier than the minimum east of the Andes. This summer minimum of LTO west of the Andes is probably due to photochemical ozone destruction in the low-NO_x and high-H_2O marine environments mentioned above. The observed tropospheric ozone at Natal, Ascension Island, and Brazzaville [*Kirchhoff et al.*, 1996; *Logan and Kirchhoff*, 1986; *Olson et al.*, 1996; *Thompson et al.*, 1996a], stations that are influenced by the same biomass-burning season (August to November) [*Hao and Liu*, 1994], shows similar seasonal behavior as the LTO east of the Andes. The consistency of the maximum LTO on both sides of the Andes with the biomass burning season suggests that the maximum LTO is linked to the biomass burning on the South American continent. *Kim and Newchurch* [1996] indicate that persistent easterly winds throughout the year over equatorial South America and persistent subsidence in the eastern Pacific Ocean are favorable for transporting the enhanced tropospheric ozone and its precursors west of the Andes. The maximum LTO east

of the Andes at 23°S south is smaller than the LTO west of the Andes and is 2 months later. At these latitudes the biomass burning is less active. Furthermore, we expect that the ozone maximum should be in phase on both sides if it is due to biomass burning. Therefore, the seasonal variation at these latitudes appears to be less influenced by biomass burning. This difference is consistent with the analysis of the National Centers for Environmental Prediction/National Center for Atmospheric Research (NCEP/NCAR) meteorological data by *Kim and Newchurch*, [1996]. The spring maximum at these latitudes is influenced by stratospheric-tropospheric exchange, which also influences Northern Hemispheric midlatitude coastal and less polluted remote regions [*Logan*, 1985; *Oltmans and Levy*, 1994; *Scheel et al.*, 1997; *Winkler*, 1988b]. The LTO in the northern equatorial tropics shows little seasonal variation on both the east (5°-10°N) and the west (3°-10°N) sides of the Andes. This seasonal behavior is consistent with the observed ozone at Panama (9°N) [*Chatfield and Harrison*, 1977] and the derived LTO at 5°-7°N by *Kim and Newchurch* [1996].

The LTO in the eastern Pacific Ocean west of the Mexican Mountains (15°-30°N, Plate 2a) is highest in the spring and lowest in the summer. East of the Mexican Mountains, the spring maximum at 15°-23°N shifts to a summer maximum (25°-30°N). The lowest ozone is in the winter. Ozone maximizes in the spring at 20°-30°N west of the Mexican Mountains, coincident with stratospheric-tropospheric exchange activities. Biomass burning peaks during the March-May period on both sides of the Mexican Mountains at 15°-25°N (Plate 1). The spring ozone maximum at 15°-25°N on both sides could be partly driven by biomass burning. The shift of the spring maximum to a summer maximum east of the Mexican Mountains coincides with the change from coastal regions to continental regions. There is less biomass burning at 25°-30°N. The summer maximum is due to photochemical ozone production in continental regions with higher NO_x and Volatile Organic Compounds (VOC) levels. This summer maximum of surface ozone or lower tropospheric ozone is found at most of the rural sites in the United States and Europe [*Logan*, 1985; *Oltmans and Levy*, 1994; *Scheel et al.*, 1997]. The summer ozone minimum is also observed at coastal sites in Florida [*Chatfield and Harrison*, 1977], Louisiana, and Texas [*Vieziee et al.*, 1982]. This summer minimum is probably due to photochemical ozone destruction in low NO_x environments. From ship-borne observations, *Winkler* [1988a] found that the surface ozone exhibits a spring maximum but a fall or winter minimum at similar latitudes in the North Atlantic Ocean. The different time period in the ozone minimum in *Winkler* [1988a] is probably due to the fact that the Atlantic Oceanic regions are subjected to polluted sources from the North American continent. At latitudes 35°-40°N we derived LTO only in the summer. According to the magnitude of LTO, it probably shows a summer maximum value on both sides of the mountains. There are large urban cities on both sides of these mountains, and the photochemical ozone production probably leads to the summer maximum.

Figure 1, with Plate 2c, indicates that the area between 6° and 20°N corresponds to east Africa west of the mountains. The area between 29° and 35°N corresponds to the northern Arabian Peninsula. LTO west of the mountains in south Sudan (Plate 2c, 6°-13°N) shows a summer minimum and a winter maximum, consistent with the scan-angle retrievals of
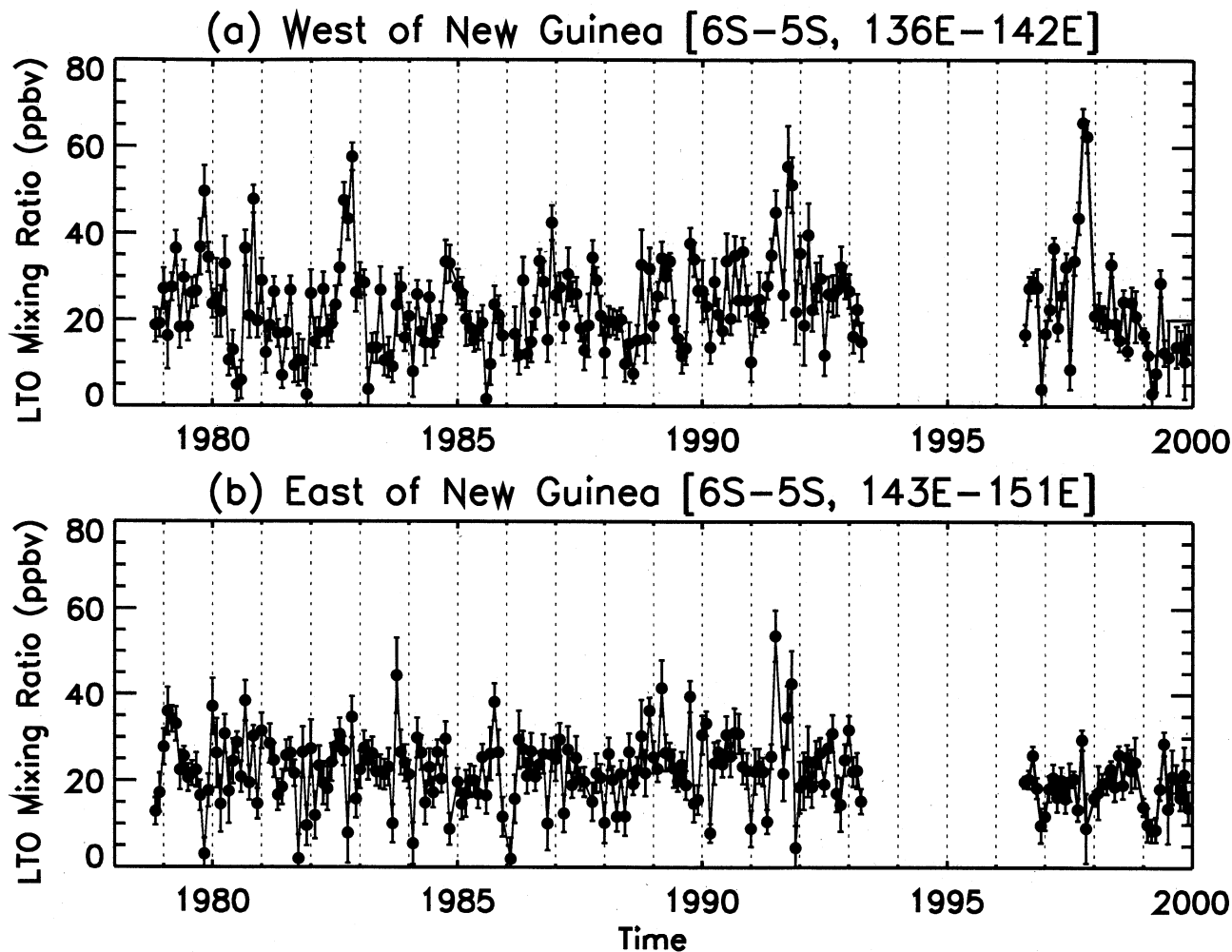
Figure 3. Time series of Lower-Tropospheric Ozone (LTO) derived from NIMBUS-7 TOMS (1978-1992) and Earth Probe TOMS (1996-2000) (a) west of New Guinea (5°-6°S, 136°-142°E) and (b) east of New Guinea (5°-6°S, 143°-151°E).

Kim et al. [2001]. This behavior is consistent with the biomass burning activity characterized by the fire maps (Plate 1). At higher latitudes in north Sudan, the Red Sea, and its west coastal regions (15°-20°N), a summer maximum (~45 ppbv) with less seasonal variation exists. The large ozone gradient at 15°N across the Sudan regions in the summer is consistent with the precipitation distribution in this region. The annual variation of precipitation from NCEP/NCAR reanalysis in 1988-1994 [*Kalnay et al.,* 1996] shows that the rainy season in south Sudan starts from March and ends in November with a peak precipitation rate of 150 mm/month in the summer. In the north Sudan region the precipitation rate is less than 40 mm/month throughout the year. Therefore, the stronger wet-deposition, convective activity, and higher water-vapor environment leads to a summer ozone minimum in the south Sudan region. In the Iraq region of the Arabian Peninsula (30°-35°N) the LTO is not complete for all months but does clearly show a broad summer maximum (50-60 ppbv) and significant seasonal variation with still high ozone (~40 ppbv) in other seasons. In the coastal region near Morocco (30°-32°N, 7°-12°W) we obtained LTO from June to December (not plotted) when the ozone dropped from about 65 ppbv in the summer to about 25 ppbv in the winter.

The surface ozone measured at the high mountain site Izaña, Canary Islands (28°N, 16°W, 2.3 km), shows a maximum of about 60 ppbv from May to July and a minimum in October of about 30 ppbv [*Oltmans and Levy,* 1994], comparable to the derived LTO near Morocco.

Plate 2d portrays South Africa between 28° and 30°S and east Africa between 0°-15°N, both east of their respective mountain ranges. At 28°-30°S east of the South Africa mountains, LTO shows a springtime maximum consistent with the biomass burning season in these regions (Plate 1) and suggested by *Olson et al.* [1999]. The LTO at 1°S-2°N in Kenya (eastern side) shows little seasonal variation about mean values of ~30 ppbv, consistent with the seasonal pattern in the northern tropics of South America. The seasonal variation at 5°N, with a summer-fall minimum is consistent with the seasonal variation on the west side of the mountains in Africa at the same latitude. Ozone amounts increase systematically ~10-15 ppbv with increasing latitude north, maintaining the same seasonal pattern.

Plate 2e and 2f show the derived LTO west and east of New Guinea, respectively. The derived LTO east of New Guinea (Pacific Ocean region) shows a small seasonal variation, highest from June to October (~24 ppbv) and lowest

from November to February (16 ppbv). This behavior is consistent with the results of *Kim and Newchurch* [1998]. West of New Guinea, our current results show the maximum LTO during September to November, about 3 months later than the *Kim and Newchurch* [1998] values. The biomass burning in New Guinea and Indonesia is different from that in South America and South Africa, where large-scale biomass burnings occur every year [*Fujiwara et al.*, 1999]. The extensive forest fires due to sparse precipitation usually take place in September to November for a period of a few years coinciding with El Niño events [*Folkins et al.*, 1997; *Fujiwara et al.*, 1999; *Komala et al.*, 1996].

Figure 3a shows the time series of monthly mean LTO at 5.5°S west of New Guinea. High ozone of ~60 ppbv occurs during September-November in 1982, 1992, and 1997, coincident with 1982-1983, 1992-1993, and 1997-1998 El Niño events. Smaller annual peaks from September to November are observed in 1979, 1980 (after 1976-1978 El Niño), 1984 (after 1982-1983 El Niño), and 1987 (1986-1987 El Niño). The LTO east of New Guinea (Figure 3b) does not show enhanced values during these periods. The enhanced ozone in the western Pacific Ocean during El Niño events could be due to both the convection pattern change and biomass burning [*Chandra et al.*, 1998]. If the LTO is due primarily to the convection pattern change, we expect to see similar increases on both sides of New Guinea. The correspondence of the derived LTO only west of New Guinea with the biomass burning seasons supports the suggestion that the enhanced ozone is, at least in part, due to photochemical production from biomass burning. Ozonesonde measurements at Java also show enhanced ozone in October 1997 (Figure 2e), which is due primarily to biomass burning in the Sumatra and Borneo islands [*Fujiwara et al.*, 2000]. As a result of consistent easterly winds at these latitudes, the enhanced ozone and its precursors are not transported east of New Guinea [*Kim and Newchurch*, 1998; *Kita et al.*, 2000] and no enhanced ozone is observed east of New Guinea.

In Plate 2h, we see high concentrations of ozone east of the Himalayas (29°-32°N, 100°-108°E, western China), highest in the spring (~70 ppbv) and lowest in the autumn and winter (~45 ppbv). The ozone west of the Himalayas (27°-33°N, 70°-84°E, northern India) in Plate 2g shows much lower ozone, with a maximum in the summer of about 40 ppbv and a minimum in the winter of about 28 ppbv. The results near the Himalayas are the most stressing of the underlying assumptions of this method. For this reason, the confidence in this geographical area is less than in the other areas. The seasonal patterns, however, are reasonable. Furthermore, the area in China with high ozone values observed by this method (Plate 2h) contains a very large industrial metropolis, Chongqing.

4. Conclusions

In this study we derived the Lower Tropospheric Ozone (LTO) using the Topographic Contrast Method (TCM) from aerosol-corrected and sea-glint-corrected TOMS high-resolution level-2 clear-sky measurements near several mountainous regions, including the Andes Mountains, the Mexican and Rocky Mountains, the mountains in Africa and the Arabian Peninsula, New Guinea, and the Himalayan Mountains. Comparing these derived LTO amounts (approximately 0-2 km) with ozonesonde observations at

Boulder, Cristobal, Fiji, and Tahiti indicates that the seasonal variation of the derived LTO agrees well with seasonal variations from these ozonesonde observations. The derived LTO provides a good opportunity for studying the seasonal variation of lower tropospheric ozone in several interesting areas of the world. The data from this study are available at http://vortex.nsstc.uah.edu/atmchem.

The influence of biomass burning is evident in the seasonal variation of LTO on both sides of the Andes Mountains between 23°S and 2°N, in southern Africa, in southern Sudan, and, especially in relation to the El Niño modulation, west of New Guinea. Also, in northern equatorial Africa consistent with the seasonality of the measured fires, we see a seasonal cycle in LTO also observed by one other satellite technique, the scan angle method [*Kim et al.*, 2001].

Similar to the ozone in the northern tropics of South America, little seasonal variation is found in Kenya (1°S - 2°N), consistent with the Nairobi ozonesonde record [*Thompson and Witte*, 1999]. In north Sudan (15°-20°N), where it is dry throughout the year and there is almost no biomass burning, we see a summer maximum and less annual variation than in the biomass burning regions. The importance of stratospheric intrusion is evident in the seasonality observed in the eastern Pacific Ocean at 15°-30°N and 30°-20°S and east of the Himalayas in western China.

In the continental regions such as west and east of the Rocky Mountains (35°-40°N), east of the Mexican Mountains (23°-30°N), Iraq, and western China, which are subject to the anthropogenic emissions of ozone precursors, high concentrations of ozone are usually found in a summer maximum. In coastal regions, such as in the eastern Pacific Ocean west of the Andes and Mexican Mountains, an ozone minimum usually occurs in the summer, suggesting photochemical ozone destruction in low NO_x and high H_2O environments. Precipitation also plays an important role in ozone loss due to stronger wet deposition, convective activity, and a high H_2O environment such as the case in south Sudan.

References

Brasseur, G.P., J.T. Kiehl, J.-F. Muller, T. Schneider, C. Granier, X.X. Tie, and D. Hauglustaine, Past and future changes in global tropospheric ozone: Impact on radiative forcing, *Geophys. Res. Lett.*, 25, 3807-3810, 1998.

Chandra, S., J.R. Ziemke, W. Min, and W.G. Read, Effects of 1997-1998 El Nino on tropospheric ozone and water vapor, *Geophys. Res. Lett.*, 25, 3867-3870, 1998.

Chatfield, R., and H. Harrison, Tropospheric ozone, 2. Variations along a meridional band, *J. Geophys. Res.*, 82, 5969-5976, 1977.

Crutzen, P.J., Tropospheric ozone: An overview, in *Tropospheric*

Ozone, Regional, and Global Scale Interaction, NATO ASI Ser., edited by I.S.A. Isaksen, and D. Reidel, pp. 3-32, Springer-Verlag, New York, 1988.

Cunnold, D.M., R.F. Weiss, R.G. Prinn, D. Hartley, P.G. Simmonds, P.J. Fraser, B. Miller, F.N. Alyea, and L. Porter, GAGE/AGAGE measurements indicating reductions in global emissions of CCl3F and CCl2F2 in 1992-1994, *J. Geophys. Res., 102,* 1259-1269, 1997.

Folkins, I., R. Chatfield, D. Baumgardner, and M. Proffitt, Biomass burning and deep convection in southeastern Asia: Results from ASHOE/MAESA, *J. Geophys. Res., 102,* 13,291-13,299, 1997.

Fujiwara, M., K. Kita, S. Kawakami, T. Ogawa, N. Komala, S. Saraspriya, and A. Suripto, Tropospheric ozone enhancements during the Indonesian forest fire events in 1994 and in 1997 as revealed by ground-based observations, *Geophys. Res. Lett., 26,* 2417-2420, 1999.

Fujiwara, M., K. Kita, T. Ogawa, S. Kawakami, T. Sano, N. Komala, S. Saraspriya, and A. Suripto, Seasonal variation of tropospheric ozone in Indonesia revealed by 5-year ground-based observations, *J. Geophys. Res., 105,* 1879-1888, 2000.

Hao, W.M., and M.-H. Liu, Spatial and temporal distribution of tropical biomass burning, *Global Biogeochem. Cycles, 8,* 495-503, 1994.

Hsu, N.C., R.D. McPeters, C.J. Seftor, and A.M. Thompson, Effect of an improved cloud climatology on the total ozone mapping spectrometer total ozone retrieval, *J. Geophys. Res., 102,* 4247-4255, 1997.

Hudson, R.D., J.-H. Kim, and A.M. Thompson, On the derivation of tropospheric column from radiances measured by the total ozone mapping spectrometer, *J. Geophys. Res., 100,* 11,137-11,145, 1995.

Jacob, D.J., J.A. Logan, G.M. Gardner, R.M. Yevich, C.M. Spivakovsky, and S.C. Wofsy, Factors regulating ozone over the United States and its export to the global atmosphere, *J. Geophys. Res., 98,* 14,817-14,826, 1994.

Jacob, D.J., J.A. Logan, and P.P. Murti, Effect of rising Asian emissions on surface ozone in the United States, *Geophys. Res. Lett., 26,* 2175-2178, 1999.

Jiang, Y., and Y.L. Yung, Concentrations of tropospheric ozone from 1979 to 1992 over tropical Pacific South America from TOMS data, *Science, 272,* 714-716, 1996.

Johnson, J.E., R.H. Gammon, J. Larsen, T.S. Bates, S.J. Oltmans, and J.C. Farmer, Ozone in the Marine Boundary Layer over the Pacific and Indian Oceans: Latitudinal gradients and diurnal cycles, *J. Geophys. Res., 95,* 11,847-11,856, 1990.

Kalnay, E., et al., The NCEP/NCAR 40-year reanalysis project, *Bull. Am. Meteorol. Soc., 77,* 437-471, 1996.

Kim, J.H., and M.J. Newchurch, Climatology and trends of tropospheric ozone over the eastern Pacific Ocean: The influences of biomass burning and tropospheric dynamics, *Geophys. Res. Lett., 23,* 3723-3726, 1996.

Kim, J.H., and M.J. Newchurch, Biomass-burning influence on tropospheric ozone over New Guinea and South America, *J. Geophys. Res., 103,* 1455-1461, 1998.

Kim, J.H., M.J. Newchurch, and K. Han, Distribution of Tropical Tropospheric Ozone determined by the scan-angle method applied to TOMS measurements, *J. Atmos. Sci., in press,* 2001.

Kirchhoff, V.W.J.H., J.R. Alves, F.R. da Silva, and J. Fishman, Observations of ozone concentrations in the Brazilian cerrado during the TRACE A field expedition, *J. Geophys. Res., 101,* 24,029-24,042, 1996.

Kita, K., M. Fujiwara, and S. Kawakami, Total ozone increase associated with forest fires over the Indonesian region and its relation to the El Nino-Southern oscillation, *Atmos. Environ., 34,* 2681-2690, 2000.

Klenk, K.F., P.K. Bhartia, A.J. Fleig, V.G. Kaveeshwar, R.D. McPeters, and P.M. Smith, Total ozone determination from the Backscattered Ultraviolet (BUV) experiment, *J. Appl. Meteorol., 21,* 1672-1684, 1982.

Komala, N., S. Saraspriya, K. Kita, and T. Ogawa, Tropospheric ozone behavior observed in Indonesia, *Atmos. Environ., 30,* 1851-1856, 1996.

Logan, J.A., Tropospheric ozone: Seasonal behavior, trends, and anthropogenic influence, *J. Geophys. Res., 90,* 10,463-10,482, 1985.

Logan, J.A., and V.W.J.H. Kirchhoff, Seasonal variations of tropospheric ozone at Natal, Brazil, *J. Geophys. Res., 91,* 7875-7881, 1986.

Marufu, L., F. Dentener, J. Lelieveld, M.O. Andreae, and G. Helas, Photochemistry of the African troposphere: Influence of biomass-burning emissions, *J. Geophys. Res., 105,* 14,513-14,530, 2000.

McPeters, R.D., et al., *Nimbus-7 Total Ozone Mapping Spectrometer (TOMS) Data Products User's Guide,* 67 pp., NASA, 1996.

McPeters, R.D., and G.J. Labow, An assessment of the accuracy of 14.5 years of Nimbus 7 TOMS Version 7 ozone data by comparison with the Dobson network, *Geophys. Res. Lett., 23,* 3695-3698, 1996.

Moxim, W.J., and H. Levy, A model analysis of the tropical South Atlantic Ocean tropospheric ozone maximum: The interaction of transport and chemistry, *J. Geophys. Res., 105,* 17,393-17,415, 2000.

Newchurch, M.J., X. Liu, and J.H. Kim, On the accuracy of TOMS retrievals over tropical cloudy regions, *J. Geophys. Res., in press,* 2001.

Olson, J.R., J. Fishman, V.W.J.H. Kirchhoff, D. Nganga, and B. Cros, Analysis of the distribution of ozone over the southern Atlantic region, *J. Geophys. Res., 101,* 24,083-24,093, 1996.

Olson, J.R., B.A. Baum, D.R. Cahoon, and J.H. Crawford, Frequency and distribution of forest, savanna, and crop fires over tropical regions during PEM-Tropics A, *J. Geophys. Res., 104,* 5865-5876, 1999.

Oltmans, S.J., and H. Levy, Surface ozone measurements from a global network, *Atmos. Environ., 28,* 9-24, 1994.

Scheel, H.E., et al., On the spatial distribution and seasonal variation of lower-troposphere ozone over Europe, *J. Atmos. Chem., 28,* 11-28, 1997.

Thompson, A.M., and J.C. Witte, SHADOZ (Southern Hemisphere Additional OZonesondes): A new data set for the Earth Science Community, *Earth Obs., 11,* 27-30, 1999.

Thompson, A.M., et al., Ozone over southern Africa during SAFARI-92/TRACE A, *J. Geophys. Res., 101,* 23,793-23,807, 1996a.

Thompson, A.M., K.E. Pickering, D.P. McNamara, M.R. Schoeberl, R.D. Hudson, J.H. Kim, E.V. Browell, V.W.J.H. Kirchhoff, and D. Nganga, Where did tropospheric ozone over southern Africa and the tropical Atlantic come from in October 1992? Insights from TOMS, GTE TRACE A, and SAFARI 1992, *J. Geophys. Res., 101,* 24,251-24,278, 1996b.

Torres, O., and P.K. Bhartia, Impact of tropospheric aerosol absorption on ozone retrieval from backscattered ultraviolet measurements, *J. Geophys. Res., 104,* 21,569-21,577, 1999.

Vieziee, W., H.B. Singh, and H. Shiegishi, The impact of stratospheric ozone on tropospheric air quality: Implications from analysis of existing field of data, *Proj. 1140,* SRI Int., Menlo Park, Calif., 1982.

Winkler, P., Meridional distribution of surface ozone over the Atlantic (83 N-76 S), *Ozone in the Atmosphere,* 1988a.

Winkler, P., Surface ozone over the Atlantic Ocean, *J. Atmos. Chem., 7,* 73-91, 1988b.

World Meteorological Organization (WMO), *Scientific Assessment of Ozone Depletion: 1998,* p. 4.16, NASA, NOAA, UNEP, WMO, EC, Geneva, Switzerland, 1999.

Ziemke, J.R., and S. Chandra, Seasonal and interannual variabilities in tropical tropospheric ozone, *J. Geophys. Res., 104,* 21,425-21,442, 1999.

X. Liu and M.J. Newchurch, Department of Atmospheric Science, University of Alabama in Huntsville, 301 Sparkman Drive, Huntsville, AL, 35805. (mike@nsstc.uah.edu)

J.H. Kim, Department of Atmospheric Science, Pusan National University, South Korea, 609-735. (jaekim@sabunim.com)